Single molecule magnets: High frequency electron paramagnetic resonance study of two isomeric forms of an Mn_{12} molecule

S. M. J. Aubin, Z. Sun, E. M. Rumberger, and D. N. Hendrickson[a)]
Department of Chemistry and Biochemistry, University of California at San Diego, La Jolla, California 92093

G. Christou
Department of Chemistry, University of Florida, Gainesville, Florida 32611-7200

Different crystallographic forms of the single molecule magnet $[Mn_{12}O_{12}(O_2CR)_{16}(H_2O)_4]$ (complex **1**) with a given *R* substituent have been isolated. The two different isomeric forms of the *p*-methylbenzoate complex crystallize as $[Mn_{12}O_{12}(O_2CC_6H_4\text{-}p\text{-Me})_{16}(H_2O)_4]\cdot(HO_2CC_6H_4\text{-}p\text{-Me})$ (complex **2**) and $[Mn_{12}O_{12}(O_2CC_6H_4\text{-}p\text{-Me})_{16}(H_2O)_4]\cdot 3H_2O$ (complex **3**). In complex **2**, one Mn^{III} ion has an abnormal Jahn–Teller distortion axis oriented at an oxide ion, and thus **2** and **3** are Jahn-Teller isomers. This reduces the symmetry of the core of complex **2** compared with that of complex **3**. Complex **2** likely has a larger tunneling matrix element and this explains why this complex shows an out-of-phase ac peak ($\chi_{M''}$) in the signal in the 2–3 K region, whereas complex **3** has its $\chi_{M''}$ peak in the 4–7 K range, i.e., the rate of tunneling of magnetization is greater in complex **2** than complex **3**. High frequency electron paramagnetic resonance (HFEPR) experiments were performed on both isomers. Computed simulations of the experimental HFEPR data yield spin Hamiltonian parameters for both complexes. © *2002 American Institute of Physics.* [DOI: 10.1063/1.1450787]

I. INTRODUCTION

Individual molecules that function as nanomagnets have been termed single-molecule magnets (SMMs).[1,2] The most thoroughly studied SMM is $[Mn_{12}O_{12}(O_2CMe)_{16}(H_2O)_4]\cdot 2(HO_2CMe)\cdot 4(H_2O)$ (complex **1**).[3,4] In order for a molecule to be a SMM it must have a large-spin ground state (S) as well as possess a large *negative* magnetoanisotropy as gauged by the axial zero-field splitting parameter D. Complex **1** has been found to have a $S=10$ ground state and significant *negative* magnetic anisotropy ($D=-0.50\ \mathrm{cm}^{-1}$). In zero-applied field, there are two equivalent lowest energy states corresponding to $m_s=-10$ and $m_s=10$ and the highest energy state corresponds to $m_s=0$. The height of the potential energy barrier is $|D|S^2=50\ \mathrm{cm}^{-1}$. In order for the magnetic moment of a Mn_{12} molecule to flip from up to down, it must either climb over the potential energy barrier in a thermally activated process or pass through the barrier by quantum tunneling.

A diagnostic technique for observing slow magnetization relaxation of a SMM is ac magnetic susceptibility. The origin of the out-of-phase peak observed for complex **1** has been the focus of considerable research.[1,4] One frequency-dependent peak is observed for complex **1** in the 4–7 K region. A puzzling observation for several Mn_{12} type molecules is that they may display two, instead of one, frequency-dependent peaks in the out-of-phase ac susceptibility response.[1] These peaks often occur in the 2–3 K (low-temperature) and 4–7 K (high-temperature) ranges. When $kT<|D|m_s^2$, the rate at which the magnetic moment of a molecule flips becomes sluggish and this relaxation phenomenon appears as an out-of-phase ac susceptibility peak within a certain range of frequencies. This leads to one out-of-phase ac signal per Mn_{12} molecule or for a collection of identical Mn_{12} molecules. However, it does *not* explain why a given complex would exhibit two out-of-phase ac signals.

II. EXPERIMENTAL RESULTS

A. ac magnetic susceptibility

In Fig. 1, the out-of-phase ac magnetic susceptibility is plotted versus temperature for complexes **2** (upper) and **3** (lower) in the temperature range of 2–10 K at frequencies of 50, 250, or 1000 Hz. These two crystallographically different forms of the *p*-methylbenzoate Mn_{12} complex each have two frequency-dependent out-of-phase ac peaks, one in the 2–3 K region and the other in the 4–7 K region. However, complex **2** has predominantly one peak in the 2–3 K region, whereas complex **3** (lower trace) has predominantly one peak in the 4–7 K region. The magnetization relaxation rates can be quantified by analyzing the frequency dependencies of the $\chi_{M''}$ signals for the two complexes as shown in Fig. 2. ac susceptibility data were collected at eight different frequencies from 1.0 to 1512 Hz for complex **3**. The data were least-squares fit to the Arrhenius equation to give $U_{eff}=64$ K. A similar analysis of the frequency dependence of the dominant low-temperature $\chi_{M''}$ peak in the ac data for complex **2** $U_{eff}=38$ K. The activation energy (U_{eff}) for reversal of the direction of the magnetization for complex **2** ($U_{eff}=38$ K) is considerably less than that ($U_{eff}=64$ K) for the isomeric complex **3**. The Mn_{12}–acetate complex **1** has been reported[3] to have a U_{eff} value of 62 K, very close to the value for complex **3**.

[a)]Electronic mail: dhendrickson@ucsd.edu

 © 2002 American Institute of Physics

Downloaded 16 May 2002 to 128.227.76.113. Redistribution subject to AIP license or copyright, see http://ojps.aip.org/japo/japcr.jsp

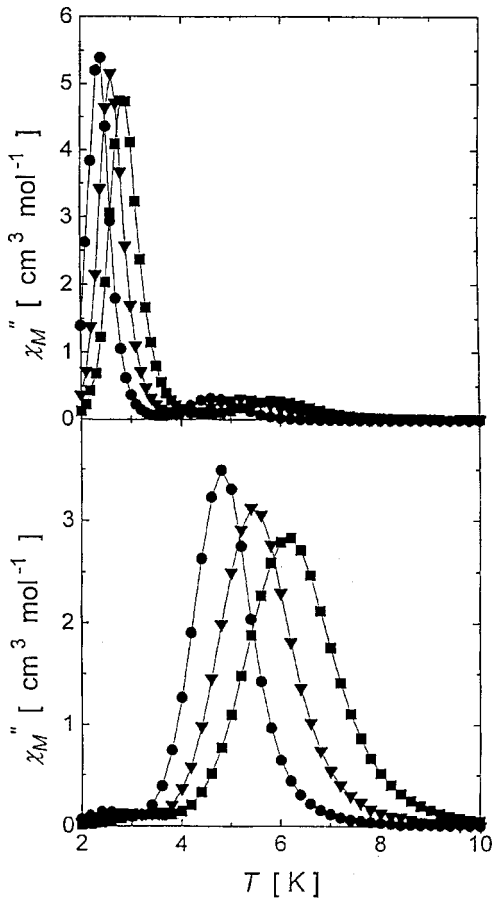

FIG. 1. Plots of $\chi_{M''}$ vs temperature for the *p*-methylbenzoate complexes **2** (upper) and **3** (lower) in an ac field of 1 G oscillating at 50 Hz (●), 250 Hz (▼), or 1000 Hz (■).

The $[Mn_{12}O_{12}]^{16+}$ cores of complexes **2** and **3** are very similar. Single crystal x-ray structures have been published elsewhere.[5] There are two distinct differences between complexes **2** and **3**, however. Complexes **2** and **3** differ in the positioning of the four H_2O and 16 carboxylate ligands. A more critical structural difference between complexes **2** and **3** is found in the orientation of the Jahn–Teller (JT) elongation axis of each Mn^{III} ion. All of the JT elongation axes in the hydrate complex **3** are roughly parallel, but they are also perpendicular to the plane of the disk-like $Mn_{12}O_{12}$ core. For complex **2**, however, one JT axis is abnormally oriented and lies in the plane of the disk-like molecule.

B. High-frequency electron paramagnetic resonance spectroscopy

High-frequency electron paramagnetic resonance (HFEPR) measurements were made to determine the ground states of the complexes **2** and **3**. Prior to the data collection, the polycrystalline samples of complexes **3** and **4** were allowed to torque in a 10 T field to ensure that the easy axis of the crystallites were oriented with the applied magnetic field. Figure 2 shows the quasi-single-crystal parallel HFEPR spectra for complex **3** (top trace collected at 30.5 K and 327.51 GHz) and for complex **2** (bottom trace collected at 29.8 K and 324 GHz). Approximately regularly spaced resonances attributed to fine structure are observed for both complexes. A comparison of the two spectra clearly illustrates that they are different. In order to estimate the spin Hamiltonian parameters for each complex, the experimental spectra were simulated. The simulation software employs a full matrix diagonalization technique to calculate the resonant magnetic fields. Full details of the simulation software can be found elsewhere.[6] The following spin Hamiltonian was used for the simulation:

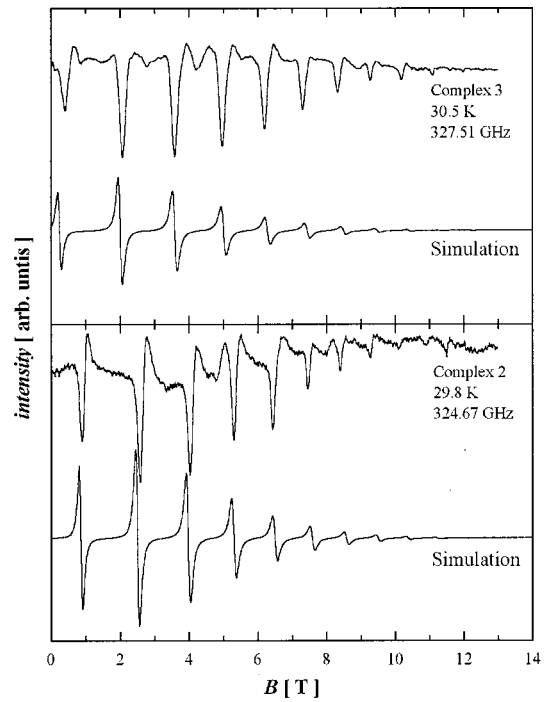

FIG. 2. HFEPR spectrum recorded at 327.51 GHz and 30.5 K for complex **3** (top). Complex **2** is shown recorded at 29.8 K and 324.67 GHz (bottom). The computed spectra (simulations) are denoted.

$$\hat{H}=g\mu_B H\times S+D\left[\hat{S}_Z^2-\frac{1}{3}S(S+1)\right]+E(\hat{S}_x^2-\hat{S}_y^2)+B_4^0\hat{O}_4^0+B_4^4\hat{O}_4^4, \quad (1)$$

where

$$\hat{O}_4^0=35S_z^4-30S(S+1)S_z^2+25S_z^2-6S(S+1)+3S^2(S+1)^2 \quad (2)$$

$$\hat{O}_4^4=\frac{1}{2}(S_+^4+S_-^4). \quad (3)$$

Figure 2 shows the computed spectra for complexes **2** and **3**. Reasonable agreement between the computed and experimental spectra were found using the parameters $S=10$, $g=1.99$, $D=-0.489\ \mathrm{cm}^{-1}$, $E=0$, and $B_4^0=-2.4\times10^{-5}\ \mathrm{cm}^{-1}$ for complex **3** and $S=10$, $g=1.99$, $D=-0.46\ \mathrm{cm}^{-1}$, $E=0$, and $B_4^0=-2.2\times10^{-5}\ \mathrm{cm}^{-1}$ for complex **2**. In both cases, inclusion of a nonzero E or B_4^4 parameter did not improve the agreement between the computed and experimental spectra. For both complexes, agreement between the computed and the experimental spectra is particularly good in the low field region (<6 T). This agreement, however, is not as rigorous in the high field region

Downloaded 16 May 2002 to 128.227.76.113. Redistribution subject to AIP license or copyright, see http://ojps.aip.org/japo/japcr.jsp

(>6 T), where the computed resonances appear at slightly lower fields. Agreement in both the low field and high field regions could be obtained if the g values were set to a value above 2.00. This possibility, however, was ruled out since g values larger than 2.00 are not expected for a mixed Mn(III)–Mn(IV) complex.

C. Origin of two out-of-phase ac susceptibility peaks

It has been shown[7] that a variety of interactions, such as a transverse quartic zero-field interaction, is important in determining the rate of magnetization tunneling. For each Mn_{12} molecule, the spin Hamiltonian given in Eq. (4) applies:

$$\hat{H}=\hat{H}_A+\hat{H}_Z+\hat{H}_{sp}+\hat{H}_T. \tag{4}$$

The first term $\hat{H}_A$ is for the axial (longitudinal) zero-field interactions, the leading terms of which are given as

$$\hat{H}_A=D\left[\hat{S}_Z^2-\frac{1}{3}S(S+1)\right]-B_4^0\hat{O}_4^0. \tag{5}$$

The parameter D is considerably larger than B_4^0 and gauges the second-order axial zero-field splitting. The second term in Eq. (4), $\hat{H}_Z$, is just the Zeeman term, which in its simplest form is given in Eq. (6):

$$\hat{H}_Z=g\mu_B\hat{H}_Z\times\hat{S}_Z. \tag{6}$$

The term $\hat{H}_{sp}$ represents the spin–phonon coupling, where a given Mn_{12} complex interacts with phonons in the crystal. The last term $\hat{H}_T$, representing transverse interactions, is the most important in terms of the rate of magnetization tunneling. Some of the larger terms in $\hat{H}_T$ are given as:

$$\hat{H}_T=g\mu_B\hat{H}_x\times\hat{S}_x+E(\hat{S}_x^2-\hat{S}_y^2)-B_4^4\hat{O}_4^4. \tag{7}$$

The transverse magnetic field $\hat{H}_x$, the rhombic zero-field operator $(\hat{S}_x^2-\hat{S}_y^2)$ and the quartic zero-field operator $\hat{O}_4^4$ mix together the m_S wave functions and this facilitates tunneling of the magnetization. There is still considerable research needed to understand this tunneling phenomenon.[8]

Complex **2** shows its out-of-phase ac susceptibility signals at essentially one half the temperature for the peaks for complex **3**. For complex **2**, it is found that $U_{eff}=38$ K, whereas complex **3** has been evaluated to have $U_{eff}=64$ K. Complex **3** behaves similarly to the high-symmetry Mn_{12}–acetate complex **1**. As described, complex **3** has all of its Mn^{III} JT distortion axes oriented nearly parallel, as in complex **1**. In contrast, the JT distortion axis at one Mn^{III} ion in complex **2** is found to be tipped $\sim 90°$ from the other axes and complex **2** thus has a lower symmetry than complex **3**. It is likely that the rhombic zero-field interactions in complex **2** are significantly larger than those in complex **3** and this means that the tunneling matrix elements for complex **2** are larger than those for complex **3**. Complex **3** behaves similarly to complex **1**.

It is unlikely that the difference in magnetization relaxation rates between complexes **2** and **3** is due to very different potential-energy barrier heights, i.e., values of U. The axial zero-field splitting parameters (D values) are similar for the two complexes as is the spin of the ground state. The rate of magnetization tunneling in complex **2** is appreciably greater than in complex **3** primarily because it is of lower molecular symmetry. The lower symmetry would increase transverse zero-field interactions, leading to a larger tunnel splitting and faster magnetization relaxation in complex **2**. It is possible that the rhombic zero-field interactions are much greater in complex **2** (see Ref. 6 for further discussion). A determination of the transverse rhombic zero-field (E) term could not be obtained by analyzing the above parallel HFEPR spectra. Detailed single-crystal HFEPR experiments are planned to determine the transverse spin Hamiltonian parameters.

ACKNOWLEDGMENTS

Two of the authors (D.N.H. and G.C.) thank the National Science Foundation for support of this research.

[1] S. M. J. Aubin, M. W. Wemple, D. M. Adams, H.-L. Tsai, G. Christou, and D. N. Hendrickson, J. Am. Chem. Soc. **118**, 7746 (1996).
[2] G. Christou, D. Gatteschi, D. N. Hendrickson, and R. Sessoli, MRS Bull. **25**, 66 (2000).
[3] R. Sessoli, D. Gatteschi, and M. Novak, Nature (London) **365**, 149 (1993).
[4] R. Sessoli, H.-L. Tsai, A. R. Schake, S. Wang, J. B. Vincent, K. Folting, D. Gatteschi, G. Christou, and D. N. Hendrickson, J. Am. Chem. Soc. **115**, 1804 (1993).
[5] S. M. J. Aubin, Z. Sun, H. J. Eppley, E. M. Rumberger, I. A. Guzei, K. Folting, P. K. Gantzel, A. L. Rheingold, G. Christou, and D. N. Hendrickon, Inorg. Chem. **40**, 2127 (2001).
[6] J. Glerup and H. Weihe, Acta Chem. Scand. **45**, 444 (1991); C. J. H. Jacobsen, E. Pedersen, J. Villadsen, and H. Weihe, Inorg. Chem. **32**, 1216 (1993).
[7] A. Caneschi, D. Gatteschi, C. Sangregorio, R. Sessoli, L. Sorace, A. Cornia, M. A. Novak, C. Paulsen, and W. J. Wernsdorfer, J. Magn. Magn. Mater. **200**, 182 (2000).
[8] A. D. Kent, Y. Zhong, L. Bokacheva, D. Ruiz, D. N. Hendrickson, and M. P. Sarachik, Europhys. Lett. **49**, 521 (2000).

Downloaded 16 May 2002 to 128.227.76.113. Redistribution subject to AIP license or copyright, see http://ojps.aip.org/japo/japcr.jsp